Volume 54
Number 33
7 September 2025
Pages 12407-12702

Dalton Transactions

An international journal of inorganic chemistry

rsc.li/dalton

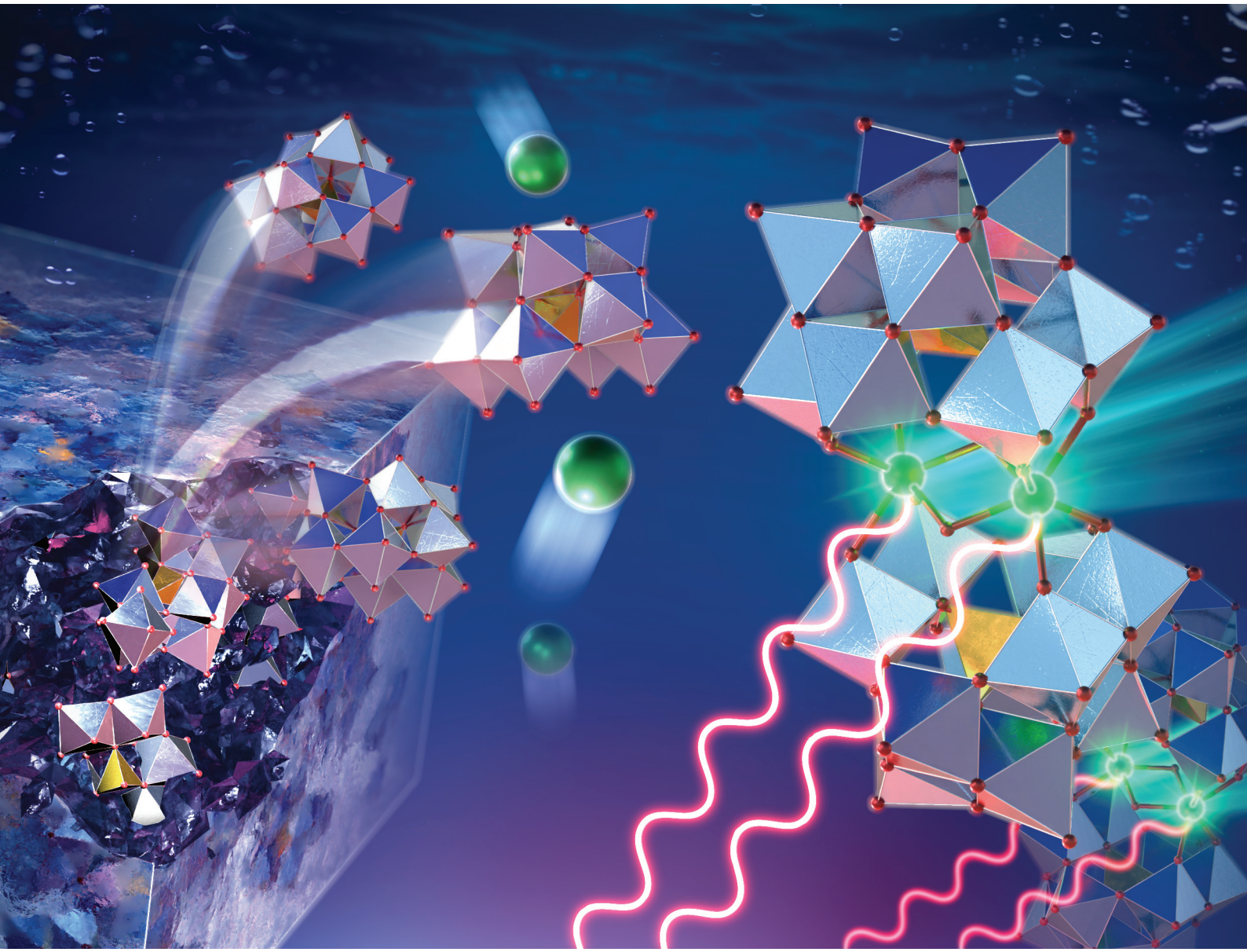

ISSN 1477-9226

ROYAL SOCIETY OF CHEMISTRY

COMMUNICATION

Ryunosuke Karashimada, Motoki Nakahara and Nobuhiko Iki
Discrete inorganic molecular upconversion: a dinuclear ytterbium–polyoxometalate complex exhibits cooperative upconversion luminescence

Dalton Transactions

ROYAL SOCIETY OF CHEMISTRY

COMMUNICATION

View Article Online
View Journal | View Issue

Cite this: *Dalton Trans.*, 2025, **54**, 12443

Received 11th June 2025,
Accepted 26th June 2025

DOI: 10.1039/d5dt01369k

rsc.li/dalton

Discrete inorganic molecular upconversion: a dinuclear ytterbium–polyoxometalate complex exhibits cooperative upconversion luminescence†

Ryunosuke Karashimada, * Motoki Nakahara and Nobuhiko Iki *

We present a novel molecular upconversion material based on a discrete lanthanide-polyoxometalate (Ln-POM) complex. A lacunary-type silicotungstate, $[\gamma\text{-}SiW_{10}O_{36}]^{8-}$ (SiW), forms a dinuclear Yb-POM complex, $[Yb_2(\mu_2\text{-}OH)_2(\gamma\text{-}SiW_{10}O_{36})_2]^{12-}$ (Yb-SiW), which exhibits upconversion luminescence *via* a cooperative luminescence mechanism in the visible region upon near-infrared excitation of its two Yb ions in CD_3CN.

A myriad of inorganic materials are utilized as luminescent materials owing to their excellent thermal and chemical stability, ease of synthesis, and resistance to non-radiative deactivation. Among the existing luminescent inorganic materials, light upconversion (UC) in lanthanide (Ln) co-doped inorganic matrices, such as oxides and fluorides, has drawn significant attention. This is due to the non-linear optical nature of UC, wherein the emission of higher-energy photons occurs upon excitation with lower-energy incident light.[1–5] UC luminescence is a unique feature for bioimaging applications, particularly owing to its ability to be excited by near-infrared (NIR) light, which allows deeper tissue penetration with minimal photodamage. However, for bio-applications, luminescent inorganic materials often require nanoscaling to improve their biocompatibility.[2,6,7]

In contrast, discrete molecular metal complexes offer an alternative strategy for achieving UC luminescence at the molecular level, distinct from nanoparticle-based systems. However, discrete molecular metal complexes also face considerable challenges, including the formation of poly- or hetero-nuclear Ln complexes having a close Ln–Ln distance and significant vibrational deactivation caused by X–H (X = C, O, N) oscillators in the ligand or solvent. To overcome these limitations, recent advances dealing with discrete metal complexes exhibiting molecular UC, such as those by Piguet (d–f heteronuclear complex), Charbonnière (supramolecular assembly), Murugesu (molecular aggregate cluster), and our laboratory (heteronuclear cluster complex), highlight the growing potential of molecular-level UC systems in this emerging field.[8–21] These discrete molecular systems emphasize the importance of controlling the coordination number and Ln–Ln distances within the molecular framework to achieve efficient UC luminescence.

Polyoxometalates (POMs) are discrete anionic inorganic clusters formed by oxo-bridged metal centers, often incorporating heteroatoms.[22–24] The unique electronic structure of POMs, coupled with their redox activity and magnetic/photophysical properties, has led to their use in various applications, such as catalysis, magnetism, and luminescence.[25,26] Among the existing POMs, lacunary-type POMs exhibit the potential to serve as anionic inorganic ligands that can coordinate with Ln ions to form Ln-POM complexes.[27,28] The Ln-POM complexes can exhibit synergistic properties arising from the interplay between the POM ligands and Ln centers. In fact, several heteronuclear Ln-POM systems have been shown to exhibit Ln-centered or UC luminescence, although most reported UC-active Ln-POM materials are either in the solid state or incorporated into nanoparticle-based MOF-type frameworks.[26,27,29]

This study aims to advance the development of Ln-POM systems at the molecular level and establish a new class of purely inorganic UC-active molecules. Some Ln-POM complexes are soluble in solution and consist only of inorganic molecules/ligands without organic ligands, forming discrete Ln-POM molecules. Suzuki *et al.* reported dinuclear Dy–POM complexes, denoted as Dy–SiW ($[Dy_2(\mu_2\text{-}OH)_2(\gamma\text{-}SiW_{10}O_{36})_2]^{12-}$, Fig. 1).[30] Two hydroxide ions bridge the two Dy^{3+} centers to form a $\{Dy(\mu_2\text{-}OH)_2Dy\}$ core, with a Dy–Dy distance of 3.6457 Å.[30] In this study, we present a new discrete dinuclear ytterbium-POM complex ($[Yb_2(\mu_2\text{-}OH)_2(\gamma\text{-}SiW_{10}O_{36})_2]^{12-}$, Yb-SiW), in which hydroxide ions similarly bridge the two Yb^{3+} centers. The Yb–Yb distance is expected to be short, based on

Graduate School of Environmental Studies, Tohoku University, 6-6-07, Aramaki-Aoba, Aoba-ku, Sendai 980-8579, Japan.
E-mail: karashimada@tohoku.ac.jp, iki@tohoku.ac.jp

†Electronic supplementary information (ESI) available: Experimental details, characterization, and photophysical properties. See DOI: https://doi.org/10.1039/d5dt01369k

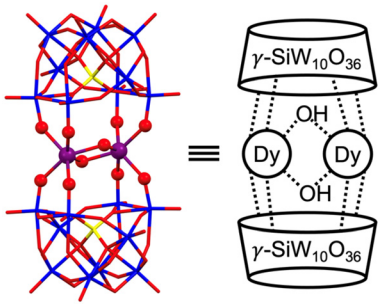

Fig. 1 Structure of the Dy–SiW complex (purple: Dy, blue: W, yellow: Si, red: O; hydrogen atoms have been omitted for clarity).[30]

the analogous Dy-SiW complex, which is favorable for UC luminescence. In fact, the designed Yb-SiW complex exhibits two distinct luminescence behaviors in acetonitrile: (i) NIR luminescence *via* energy transfer and (ii) visible UC luminescence driven by cooperative luminescence (CL).

The Yb-SiW complex was synthesized according to a previously reported procedure and characterized by Fourier-transform infrared (FT-IR) spectroscopy, elemental analysis, and electrospray ionization mass spectrometry (ESI-MS).[30,31] The FT-IR spectra (Fig. S1†) and elemental analysis supported the formation of the Yb-SiW complex. Furthermore, ESI-MS analysis confirmed the presence of the Yb-SiW complex in acetonitrile solution, showing an isotopic distribution centered at *m*/*z* 2645.21595, which could be assigned to $[2Yb^{3+} + 2(\gamma\text{-}SiW_{10}O_{36})^{8-} + 11TBA^{+} + 4H^{+} + 2OH^{-}]^{3+}$ (*m*/*z* 2645.2183, TBA^{+}: tetrabutylammonium). The experimental results collectively confirm the successful synthesis and presence of the Yb-SiW complex in acetonitrile solution. As a non-emissive reference, the Lu–SiW complex was also prepared and analyzed similarly, confirming its formation (Fig. S1 and S3†).

The Yb-SiW complex in acetonitrile solution exhibited a sharp emission band at 980 nm, corresponding to the $^2F_{5/2} \rightarrow {}^2F_{7/2}$ transition of the Yb^{3+} ion (Fig. 2). The excitation spectrum of the Yb-SiW complex showed a broad band below 350 nm,

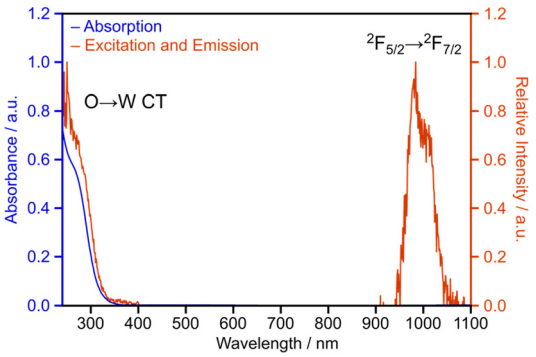

Fig. 2 Absorption (blue), excitation (red), and emission (red) spectra of the Yb-SiW complex in CH_3CN. Absorption spectrum: [Yb-SiW] = 11 μM, excitation and emission spectra: [Yb-SiW] = 14 μM, λ_{ex} = 260 nm, λ_{em} = 980 nm.

which is consistent with its absorption spectrum (Fig. 2). These bands were attributed to the O → W charge-transfer transitions within the silicotungstate ligand, $(\gamma\text{-}SiW_{10}O_{36})^{8-}$. These observations indicate that the observed NIR luminescence originates from the energy transfer between the POM ligand and the Yb^{3+} center.

The luminescence decay curve of Yb-centered luminescence fitted well using a single-exponential function (Fig. S4†), suggesting that the NIR emission from the Yb-SiW complex in acetonitrile originates from a single component. The observed luminescence lifetime (τ_{obs}) was determined as 1.27 μs, which falls within the range of lifetimes associated with long-lived Ln-centered luminescence. Moreover, the radiative luminescence lifetime (τ_{rad}) of the Yb center was estimated to be 0.593 ms based on the absorption spectrum of the $^2F_{5/2} \leftarrow {}^2F_{7/2}$ transition (Fig. S5†). Next, the quantum yield of the Yb center (ϕ_{Yb}) in the Yb-SiW complex was calculated using the following equation (eqn (1)):

$$\phi_{Yb} = \tau_{obs}/\tau_{rad}, \quad (1)$$

yielding a value of 0.21%. The ϕ_{Yb} value of the Yb-SiW complex was approximately one order of magnitude lower than those of other cooperative UC systems, including dinuclear complexes (ϕ_{Yb} = 1.7, 2.6%),[15] supramolecular assemblies (ϕ_{Yb} = 1.5, 2.3%),[14,32] and nonanuclear cluster complexes (ϕ_{Yb} = 1.7, 2.1, 2.6%).[12,13,20] It should be noted that the τ_{rad} values of the Yb-SiW complex and other existing cooperative UC systems are similar (typically 0.5–1.13 ms); therefore, a relatively lower ϕ_{Yb} value of the Yb-SiW complex can be attributed to its shorter τ_{obs}. The shorter τ_{obs} of the Yb-SiW complex indicates the presence of nonradiative deactivation pathways, such as high-energy O–H vibrations within the $\{Yb(\mu_2\text{-}OH)_2Yb\}$ core or intrinsic vibrational modes of the SiW ligand in the Yb-SiW complex.

Although the Yb^{3+} centers contain O–H groups, the presence of two Yb^{3+} centers in close proximity in the Yb-SiW complex makes it a promising candidate for CL-based visible emission. Upon NIR laser excitation, the Yb-SiW complex in CD_3CN exhibited visible emission at 488 nm (Fig. 3a). To rule out the contribution of any alternative sources behind the emission at 488 nm, control experiments were conducted using only the CD_3CN solvent in the absence of the Yb-SiW complex. The CD_3CN solvent showed a weak background signal with a slope of approximately one in a log–log plot of the signal at 488 nm *versus* excitation power, consistent with the scattering of the excitation light (Fig. S6†). After subtracting the background contribution, the corrected emission intensity of the Yb-SiW complex *versus* excitation power yielded a slope of approximately two in the log–log plot, indicating that the 488 nm emission proceeds *via* a two-photon excitation process (Fig. 3b). Since the $\{Ln\text{–}\mu_2OH\text{–}Ln\}$ unit in a structurally related Ln-SiW complex has been reported to exhibit an intermetallic distance of 3.6457 Å (for Ln = Dy), the Yb-SiW complex is expected to possess a comparable Yb–Yb distance. According to Auzel's criterion, observation of CL

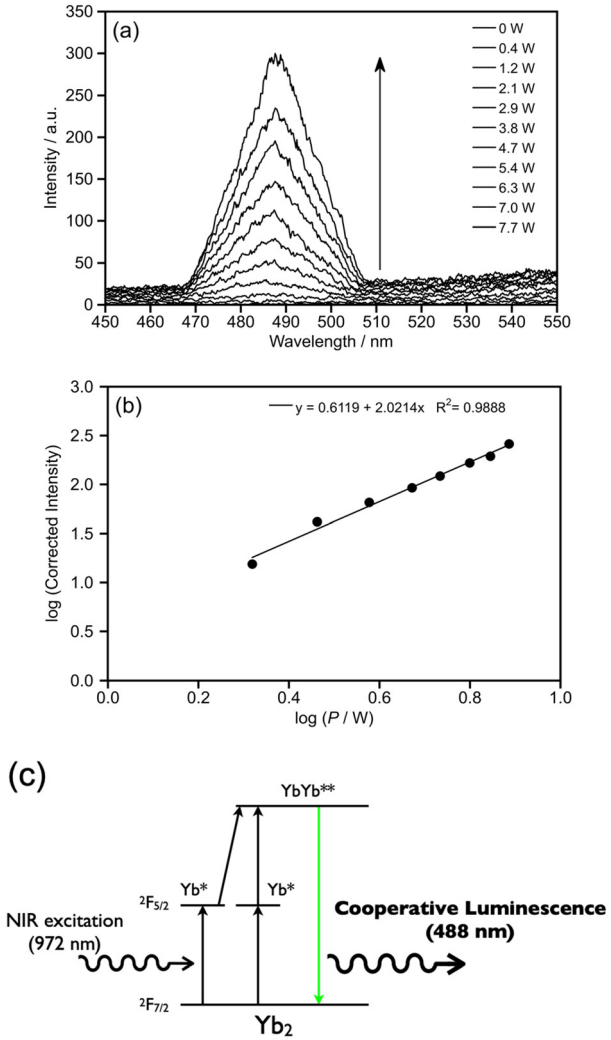

Fig. 3 (a) CL spectra of the Yb-SiW complex in CD_3CN, (b) log–log plot of the emission intensity at 488 nm *versus* the excitation power of the NIR laser, and (c) mechanism of CL. [Yb-SiW] = 3.0 mM, λ_{ex} = 972 nm.

requires Ln–Ln distances below 5 Å,[33] which supports the feasibility of a CL mechanism in the Yb-SiW complex (Fig. 3c). Furthermore, the absence of residual emissions in the corrected emission spectra of the free SiW ligand and the Lu–SiW complex confirms that the 488 nm band emitted by the Yb-SiW complex in CD_3CN is attributable to UC involving two Yb^{3+} ions (Fig. S7†). We are currently attempting to obtain direct structural data on the Yb–Yb distance in the Yb-SiW complex, which will be reported in future work.

In summary, we have synthesized and characterized a discrete dinuclear Yb-SiW complex that exhibits UC luminescence in CD_3CN. The UC emission is attributed to a CL mechanism, as supported by the excitation power dependence and the presence of two Yb^{3+} centers. The Yb-SiW complex represents a fully inorganic, molecularly discrete system composed entirely of inorganic components without any organic ligands. These findings pave the way for the rational design of UC-active materials based on discrete Ln-POM architectures. Given that Ln-SiW systems can form heteronuclear complexes (LnLn′–SiW),[34] we are currently extending this approach for developing heteronuclear Ln-POM systems with tunable UC luminescence.

Conflicts of interest

There are no conflicts to declare.

Data availability

The data supporting this article have been included as part of the ESI.†

Acknowledgements

We thank Mr Shunsuke Kayamori and Mr Hiroyuki Momma for the ESI-MS measurements. We thank Dr Tatsuo Nakagawa and Mr Hiroaki Hanada for the measurements of the luminescence decay curve. This work was supported by JSPS KAKENHI (grant numbers: 20K15308 and 23K04801).

References

1 F. Auzel, *Chem. Rev.*, 2004, **104**, 139–173.
2 M. Haase and H. Schafer, *Angew. Chem., Int. Ed.*, 2011, **50**, 5808–5829.
3 X. Huang, S. Han, W. Huang and X. Liu, *Chem. Soc. Rev.*, 2013, **42**, 173–201.
4 J. Zhou, Q. Liu, W. Feng, Y. Sun and F. Li, *Chem. Rev.*, 2014, **115**, 395–465.
5 B. S. Richards, D. Hudry, D. Busko, A. Turshatov and I. A. Howard, *Chem. Rev.*, 2021, **121**, 9165–9195.
6 Z. Zhang, S. Shikha, J. Liu, J. Zhang, Z. Mei and Y. Zhang, *Anal. Chem.*, 2019, **91**, 548–568.
7 R. Medishetty, J. K. Zareba, D. Mayer, M. Samoc and R. A. Fischer, *Chem. Soc. Rev.*, 2017, **46**, 4976–5004.
8 L. J. Charbonnière, *Dalton Trans.*, 2018, **47**, 8566–8570.
9 B. Golesorkhi, H. Nozary, A. Fürstenberg and C. Piguet, *Mater. Horiz.*, 2020, **7**, 1279–1296.
10 A. M. Nonat and L. J. Charbonnière, *Coord. Chem. Rev.*, 2020, **409**, 213192–213208.
11 B. Golesorkhi, I. Taarit, H. Bolvin, H. Nozary, J.-R. Jiménez, C. Besnard, L. Guénée, A. Fürstenberg and C. Piguet, *Dalton Trans.*, 2021, **50**, 7955–7968.
12 R. C. Knighton, L. K. Soro, A. Lecointre, G. Pilet, A. Fateeva, L. Pontille, L. Francés-Soriano, N. Hildebrandt and L. J. Charbonnière, *Chem. Commun.*, 2021, **57**, 53–56.
13 R. C. Knighton, L. K. Soro, L. Francés-Soriano, A. Rodríguez-Rodríguez, G. Pilet, M. Lenertz, C. Platas-Iglesias, N. Hilderbrandt and L. J. Charbonnière, *Angew. Chem., Int. Ed.*, 2022, **61**, e202113114.

14 R. C. Knighton, L. K. Soro, W. Thor, J. M. Strub, S. Cianferani, Y. Mely, M. Lenertz, K. L. Wong, C. Platas-Iglesias, F. Przybilla and L. J. Charbonniére, *J. Am. Chem. Soc.*, 2022, **144**, 13356–13365.
15 L. K. Soro, R. C. Knighton, F. Avecilla, W. Thor, F. Przybilla, O. Jeannin, D. Esteban-Gomez, C. Platas-Iglesias and L. J. Charbonnière, *Adv. Opt. Mater.*, 2022, **11**, 2202307–2202313.
16 D. A. Galico, C. M. Santos Calado and M. Murugesu, *Chem. Sci.*, 2023, **14**, 5827–5841.
17 L. J. Charbonnière, A. M. Nonat, R. C. Knighton and L. Godec, *Chem. Sci.*, 2024, **15**, 3048–3059.
18 D. A. Gálico, A. A. Kitos, R. Ramdani, J. S. Ovens and M. Murugesu, *J. Am. Chem. Soc.*, 2024, **146**, 26819–26829.
19 D. A. Gálico and M. Murugesu, *J. Mater. Chem. C*, 2024, **12**, 15413–15417.
20 S. P. K. Panguluri, E. Jourdain, P. Chakraborty, S. Klyatskaya, M. M. Kappes, A. M. Nonat, L. J. Charbonniére and M. Ruben, *J. Am. Chem. Soc.*, 2024, **146**, 13083–13092.
21 R. Karashimada, K. Musha and N. Iki, *Chem. Commun.*, 2025, **61**, 5110–5113.
22 M. T. Pope, in *Handbook on the Physics and Chemistry of Rare Earths*, Elsevier, 2008, vol. 38, ch. 240, pp. 337–382.
23 N. I. Gumerova and A. Rompel, *Chem. Soc. Rev.*, 2020, **49**, 7568–7601.
24 T. Ueda, *Anal. Sci.*, 2021, **37**, 107–118.
25 Y. Zhou, G. Chen, Z. Long and J. Wang, *RSC Adv.*, 2014, **4**, 42092–42113.
26 X. Xu, Y. Guo, B. Li, Y. Lv, Z. Wu, S. Liang, L. He and Y.-F. Song, *Coord. Chem. Rev.*, 2025, **522**, 216210–216228.
27 K. Zheng and P. Ma, *Dalton Trans.*, 2024, **53**, 3949–3958.
28 X. Ma, W. Yang, L. Chen and J. Zhao, *CrystEngComm*, 2015, **17**, 8175–8197.
29 S. Bej, X. Wang, J. Zhang, X. Yang and P. Ren, *Coord. Chem. Rev.*, 2024, **513**, 215862–215888.
30 K. Suzuki, R. Sato and N. Mizuno, *Chem. Sci.*, 2013, **4**, 596–600.
31 K. Kamata, K. Yonehara, Y. Sumida, K. Yamaguchi, S. Hikichi and N. Mizuno, *Science*, 2003, **300**, 964–966.
32 L. K. Soro, C. Charpentier, F. Przybilla, Y. Mély, A. M. Nonat and L. J. Charbonnière, *Chemistry*, 2021, **3**, 1037–1046.
33 F. Auzel, D. Meichenin, F. Pellé and P. Goldner, *Opt. Mater.*, 1994, **4**, 35–41.
34 R. Sato, K. Suzuki, M. Sugawa and N. Mizuno, *Chem. – Eur. J.*, 2013, **19**, 12982–12990.